Influence of Moving Internal Parts on Angular Motion of Spinning Projectiles

Charles H. Murphy*
Ballistic Research Lab., U.S. Army Armament Research and Development Command, Aberdeen Proving Ground, Md.

Projectiles containing movable internal components, when compared with rigid but otherwise equivalent projectiles, have been observed to have different damping rates, range losses, and rapid spin-downs. Two types of internal parts motion are considered: 1) linear motion of the centers of mass of the components relative to the external shell center of mass, and 2) angular motion of the components' spin axes with respect to the external shell spin axis. Motions at the projectile's pitching and yawing frequencies are considered, and such motions are shown to explain the observed flight behavior.

Nomenclature

$A_{l_p} = \frac{1}{2}\rho Sl^2 VC_{l_p}$
$A_{p\alpha} = \frac{1}{2}\rho Sl^2 V[p_b C_{M_{p\alpha}} + (L_{x0}/ml^2)C_{L_\alpha}]$
$A_q = \frac{1}{2}\rho Sl^2 V[C_{M_q} + C_{M_{\dot\alpha}} - (I_t/ml^2)C_{L_\alpha}]$
$A_\alpha = \frac{1}{2}\rho SlV^2 C_{M_\alpha}$
$B_\gamma = I_{xc}p_c - I_{tc}\dot\theta$
$B_{\gamma l} = I_{xc}p_c - I_{tc}\dot\phi_l$
C_l = $B_{\gamma l}\gamma\cos\phi_\gamma + m_c x_c \dot\phi_l \epsilon\cos\phi_\epsilon$
C_{l_p} = roll damping moment coefficient
C_{L_α} = lift force coefficient
$C_{M_{p\alpha}}$ = Magnus moment coefficient
$C_{M_q}, C_{M_{\dot\alpha}}$ = damping moment coefficients
C_{M_α} = static moment coefficient
$\boldsymbol{e}_1, \boldsymbol{e}_2, \boldsymbol{e}_3$ = unit vectors in the nonrolling aeroballistic system, $\boldsymbol{e}_1$ along the body's axis of symmetry
$\boldsymbol{e}_{1c}, \boldsymbol{e}_{2c}, \boldsymbol{e}_{3c}$ = unit vectors in the internal component's coordinate system, $\boldsymbol{e}_{1c}$ along the internal component's axis of symmetry and $\boldsymbol{e}_{3c}$ normal to $\boldsymbol{e}_1$
$E = m_c x_c \dot\theta \epsilon \exp(i\theta_\epsilon)$
h = x component of the vector between the center of mass (c.m.) of the body and the c.m. of the component
I_t = transverse moment of inertia of the projectile
I_x = axial moment of inertia of the projectile
I_{xb}, I_{tb} = axial and transverse moments of inertia of the body
I_{xc}, I_{tc} = axial and transverse moments of inertia of the internal component
K_j = length of the jth modal arm, $j = 1, 2$
l = reference length
$\boldsymbol{L}$ = angular momentum vector of the projectile
$\boldsymbol{L}_b, \boldsymbol{L}_c$ = angular momentum vector of the body and internal component, respectively
$L_{x0} = I_{xb}p_b + I_{xc}p_c$
m = mass of the projectile, $m_b + m_c$
m_b = mass of the body
m_c = mass of the internal component
$M_x, M_{\tilde y}, M_{\tilde z}$ = components of the aerodynamic moment vector in the nonrolling aeroballistic system
p, q, r = components of the projectile's angular velocity in the missile-fixed coordinate system
$p, \tilde q, \tilde r$ = components of the projectile's angular velocity in the nonrolling aeroballistic system
$p_b = \dot\phi_b$, roll rate of the body
$p_c = \dot\phi_c + \dot\theta$, roll rate of the internal component
$Q = \tilde q + i\tilde r$
$\hat r_b$ = distance of the body submass dm from the $\boldsymbol{e}_1$ axis
$\boldsymbol{r}_b$ = vector from the c.m. of the projectile to the c.m. of the body
$\boldsymbol{R}_b$ = vector from the c.m. of the body to the submass dm of the body
$\hat r_c$ = distance of the internal component submass dm from the $\boldsymbol{e}_{1c}$-axis
$\boldsymbol{r}_c$ = vector from the c.m. of the projectile to the c.m. of the internal component
$\boldsymbol{R}_c$ = vector from the c.m. of the internal component to the submass dm of the component
S = reference area
$S_l = B_{\gamma l}\gamma\sin\phi_\gamma + m_c x_c \dot\phi_l \epsilon\sin\phi_\epsilon$
t = time
V = magnitude of the velocity vector
$x_b, \hat x_b, x_c$ = $\boldsymbol{e}_1$-component of $\boldsymbol{r}_b$, $\boldsymbol{R}_b$, and $\boldsymbol{r}_c$, respectively
$\hat x_c$ = $\boldsymbol{e}_{1c}$-component of $\boldsymbol{R}_c$
$\tilde\alpha, \tilde\beta$ = angles of attack and sideslip in the nonrolling aeroballistic system
γ = the cant angle – the angle between the axis of symmetry of the internal component and the axis of symmetry of the body
$\Gamma = B_{\gamma}\gamma\exp(i\theta_\gamma)$
$\delta = |\xi|$
$\Delta\dot\phi_j = \dot\phi_j - \dot\phi_{jr}$, $j = 1, 2$
ϵ = $\epsilon_b + \epsilon_c$, the nondimensional radius of the circular motion performed by the c.m. of the internal component about the axis of symmetry of the body
$\epsilon_b = m_c\epsilon/m$
$\epsilon_c = m_b\epsilon/m$
θ = orientation angle of the angle-of-attack plane with respect to the aeroballistic axes ($\delta e^{i\theta} = \tilde\xi$)
θ_γ = orientation angle of the cant plane with respect to the aeroballistic axes
θ_ϵ = polar angle of the circular motion performed by the c.m. of the internal component about the axis of symmetry of the body
λ_j = jth damping rate ($\dot K_j/K_j$) for a rigid projectile, $j = 1, 2$
$\tilde\xi$ = $\tilde\beta + i\tilde\alpha$, the complex angle of attack

Received Feb. 14, 1977; presented as Paper 77-1138 at the AIAA 4th Atmospheric Flight Mechanics Conference, Hollywood, Fla., Aug. 8-10, 1977; revision received Oct. 31, 1977.

Index categories: LV/M Dynamics and Control; Entry Vehicle Dynamics and Control.

*Chief, Launch and Flight Division. Associate Fellow AIAA.

ρ = air density
ϕ_b = polar angle in the $e_2 - e_3$ plane of the body submass
ϕ_c = polar angle in the $e_{2c} - e_{3c}$ plane of the internal component submass
ϕ_j = $\phi_{j0} + \dot{\phi}_j t$, the orientation angle of the jth modal arm, $j = 1,2$
ϕ_{j0} = initial orientation angle of the jth modal arm, $j = 1,2$
$\hat{\phi}$ = $\phi_1 - \phi_2$
$\dot{\phi}_j$ = frequency of the jth modal arm, $j = 1, 2$ (it is assumed that $\dot{\phi}_1 > \dot{\phi}_2$, i.e., the 1-arm is the fast arm)
$\dot{\phi}_{jr}$ = frequency of the jth modal arm for a rigid projectile, $j = 1, 2$
ϕ_γ = $\theta_\gamma - \theta$
ϕ_ϵ = $\theta_\epsilon - \theta$
ω = angular velocity of the projectile
Ω = angular velocity of the nonrolling aeroballistic coordinate system

Subscripts

b,c = body, internal component
$x,\tilde{y},\tilde{z}$ = vector components in the nonrolling aeroballistic system

Special Notation

$(\dot{})$ $d(\ )/dt$

Introduction

IN 1955, four shell types exhibited unusual behavior which involved the movement of their internal parts. Three of these shells – the 20-mm M282E1, the 20-mm T216E1, and the 30-mm T306E10 – showed much less fast-mode damping when fired with the M505 fuze.[1-3] This fuze has a spherical arming rotor in a cylindrical cavity with small but nonzero clearances. The fourth shell – the 8-in. T317 – showed significant range losses and very large spin decays.[4] This shell has several rings held on a central column but free to move with small but nonzero clearances. In all these cases, small amplitude motions of the internal parts had significant effect on the parent shell's motion.

Two types of internal parts motion are possible: 1) linear movements† of their centers of mass (c.m.) relative to the external shell c.m., and 2) angular motion of their spin axes with respect to the external shell spin axis. In order that these internal movements have a significant effect on the shell motion, they must have components at the same frequencies as the shell's pitching and yawing motion. Thus, we have an internal resonance situation, but the amplitude of the internal movement is bounded. This paper develops the theory for internal motions that have a fixed phase with respect to the angle-of-attack plane. A solution is obtained for the simplifying approximation that the internal motions have a fixed phase with respect to the plane of the higher frequency component of the pitching and yawing motion. These results are used to explain the observed behavior of the four 1955 shell.

Theory

A missile-fixed coordinate system can be defined with the x axis along the missile axis of symmetry, the z axis initially pointed down and rolling with the missile, and the y axis determined by the right-hand rule. The angular velocity of the missile in these coordinates is

$$\omega = (p,\ q,\ r) \tag{1}$$

†Hodapp[5] has derived general equations for this motion, but applied them to the very simple case of longitudinal motion of a mass on the shell's axis of symmetry.

For the motion of symmetric missiles, a much more convenient coordinate system is the aeroballistic system, which pitches and yaws with the missile but has zero roll rate. Unit vectors along aeroballistic axes will be denoted as e_1, e_2, and e_3. Then, e_1 is a unit vector along the missile's axis of symmetry, while e_2 and e_3 are unit vectors perpendicular to the missile's axis of symmetry and moving in such a way that the angular velocity of the coordinate system has zero spin component. Thus, the angular velocity vector of the aeroballistic coordinate system can be expressed in missile-fixed coordinates as

$$\Omega = (0,\ q,\ r) \tag{2}$$

Transverse components of a vector in the nonrolling coordinates will be identified by tilde superscripts. In aeroballistic coordinates, the two angular velocity vectors assume the form

$$\omega = pe_1 + \tilde{q}e_2 + \tilde{r}e_3 \tag{3}$$

$$\Omega = \tilde{q}e_2 + \tilde{r}e_3 \tag{4}$$

It is important to note that for small angular motion, if e_3 is initially in the vertical plane containing the velocity vector, it will stay quite near this plane. For larger motion, the location of e_3 can be computed.[6]

We now consider the projectile to consist of its external symmetric body with mass m_b and an internal symmetric component of mass m_c, which is free to move perpendicular to the body's axis of symmetry. The axis of symmetry of the internal mass is assumed to cant at constant angle γ with respect to the body's axis of symmetry, and the plane of this cant angle is assumed to maintain a constant phase angle ϕ_γ with the angle-of-attack plane (Fig. 1). If θ and θ_γ are the orientation angles of the angle-of-attack plane and the cant plane, respectively, then

$$\theta_\gamma = \theta + \phi_\gamma \tag{5}$$

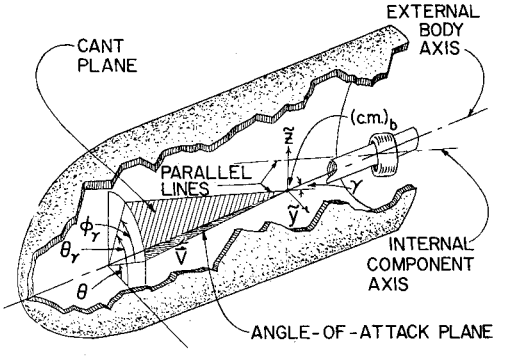

Fig. 1 Canted ring configuration, showing the cant angle γ and the orientation angle θ_γ.

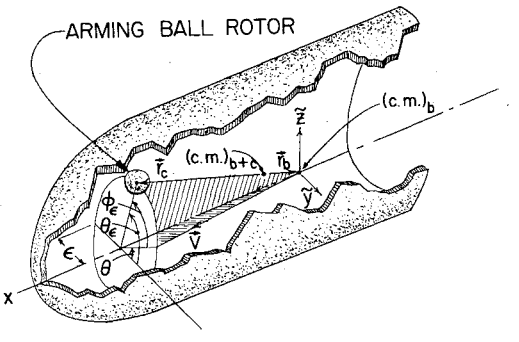

Fig. 2 Ball fuze configuration, showing the circular motion radius ϵ, the polar angle θ_ϵ and the position vectors of the body c.m. and the component c.m. relative to the body-plus-component c.m.

The motion of the c.m. of the internal component will be assumed to be a circular motion of amplitude ϵ and constant phase angle ϕ_ϵ with respect to the angle-of-attack plane. If the vectors locating the c.m. of the component and body with respect to the body-plus-internal-component c.m. are denoted by r_c and r_b, this motion of the component relative to the body (Fig. 2) is specified by the vector equation

$$r_c - r_b = he_1 - \epsilon(e_2 \cos\theta_\epsilon + e_3 \sin\theta_\epsilon) \tag{6}$$

$$\theta_\epsilon = \theta + \phi_\epsilon \tag{7}$$

Since these vectors are defined in terms of the c.m. of the combination,

$$m_b r_b + m_c r_c = 0 \tag{8}$$

and, therefore,

$$r_b = x_b e_1 + \epsilon_b(e_2 \cos\theta_\epsilon + e_3 \sin\theta_\epsilon) \tag{9}$$

$$r_c = x_c e_1 - \epsilon_c(e_2 \cos\theta_\epsilon + e_3 \sin\theta_\epsilon) \tag{10}$$

where

$$x_c = m_b h/m \qquad x_b = -m_c h/m$$
$$\epsilon_c = m_b \epsilon/m \qquad \epsilon_b = m_c \epsilon/m$$

The angular momentum vector of the body, L_b, can now be computed from its definition[7] in terms of a large number of small submasses, dm, with position vectors $r_b + R_b$.

$$L_b = \int (r_b + R_b) \times (\dot{r}_b + \dot{R}_b)\,\mathrm{d}m = m_b r_b \times \dot{r}_b + \int (R_b \times \dot{R}_b)\,\mathrm{d}m \tag{11}$$

The rotational symmetry of the body can be best exploited by expressing the position vectors of the submasses in cylindrical coordinates:

$$R_b = \hat{x}_b e_1 + \hat{r}_b[e_2 \cos\phi_b + e_3 \sin\phi_b] \tag{12}$$

Since the body is spinning with respect to the aeroballistic axes, it should be noted that $\dot{\phi}_b$ is not zero. The derivatives of r_b and R_b can, however, be easily computed using the relation

$$\dot{e}_j = \Omega \times e_j \tag{13}$$

The angular momentum can be computed from Eqs. (9) and (11-13) and simplified by neglecting terms involving ϵ_b^2.

$$L_b = L_{xb} e_1 + L_{\bar{y}b} e_2 + L_{\bar{z}b} e_3 \tag{14}$$

where the L_{jb}'s are defined in Table 1.

The angular momentum of the internal component can be computed in a similar way:

$$L_c = m_c r_c \times \dot{r}_c + \int R_c \times \dot{R}_c\,\mathrm{d}m \tag{15}$$

The integral in Eq. (15) can best be treated by the introduction of axes that pitch and yaw with the internal component. These axes can be selected so that they are principal axes of inertia for the internal component, and can be obtained from the aeroballistic axes by a rotation in roll of θ_γ about the x axis followed by a rotation in pitch of γ. For small values of γ, unit vectors along these component axes are given in terms of the e_j's by

$$e_{1c} = e_1 + \gamma(e_2 \cos\theta_\gamma + e_3 \sin\theta_\gamma) \tag{16}$$

$$e_{2c} = -\gamma e_1 + e_2 \cos\theta_\gamma + e_3 \sin\theta_\gamma \tag{17}$$

$$e_{3c} = -e_2 \sin\theta_\gamma + e_3 \cos\theta_\gamma \tag{18}$$

Table 1 Angular momentum components

$L_{xb} = I_{xb} p_b$	$+ m_c x_c \epsilon_b (\tilde{q} \cos\theta_\epsilon + \tilde{r} \sin\theta_\epsilon)$
$L_{\bar{y}b} = (I_{tb} + m_b x_b^2)\tilde{q}$	$+ m_c x_c \epsilon_b \dot{\theta} \cos\theta_\epsilon$
$L_{\bar{z}b} = (I_{tb} + m_b x_b^2)\tilde{r}$	$+ m_c x_c \epsilon_b \dot{\theta} \sin\theta_\epsilon$
$L_{xc} = I_{xc} p_c$	$+ m_c x_c \epsilon_c (\tilde{q} \cos\theta_\epsilon + \tilde{r} \sin\theta_\epsilon)$
	$+ (I_{xc} - I_{tc})\gamma(\tilde{q} \cos\theta_\gamma + \tilde{r} \sin\theta_\gamma)$
$L_{\bar{y}c} = (I_{tc} + m_c x_c^2)\tilde{q}$	$+ m_c x_c \epsilon_c \dot{\theta} \cos\theta_\epsilon + B_\gamma \gamma \cos\theta_\gamma$
$L_{\bar{z}c} = (I_{tc} + m_c x_c^2)\tilde{r}$	$+ m_c x_c \epsilon_c \dot{\theta} \sin\theta_\epsilon + B_\gamma \gamma \sin\theta_\gamma$
$L_x = L_{x0}$	$+ m_c x_c \epsilon (\tilde{q} \cos\theta_\epsilon + \tilde{r} \sin\theta_\epsilon)$
	$+ (I_{xc} - I_{tc})\gamma(\tilde{q} \cos\theta_\gamma + \tilde{r} \sin\theta_\gamma)$
$L_{\bar{y}} = I_t \tilde{q}$	$+ m_c x_c \epsilon \dot{\theta} \cos\theta_\epsilon + B_\gamma \gamma \cos\theta_\gamma$
$L_{\bar{z}} = I_t \tilde{r}$	$+ m_c x_c \epsilon \dot{\theta} \sin\theta_\epsilon + B_\gamma \gamma \sin\theta_\gamma$
$L_{x0} = I_{xb} p_b + I_{xc} p_c$	$I_t = I_{tb} + I_{tc} + m_b x_b^2 + m_c x_c^2$

The position vector of the internal component's submasses can now be given in cylindrical coordinates and the e_{jc} unit vectors.

$$R_c = \hat{x}_c e_{1c} + \hat{r}_c[e_{2c} \cos\phi_c + e_{3c} \sin\phi_c] \tag{19}$$

The derivative of this vector is somewhat more complicated than the derivative of R_b, since a term involving the precession rate $\dot{\theta}$ is present. The angular momentum of the internal component can be computed from Eqs. (10) and (15-19) and simplified by neglecting terms in ϵ_c^2.

$$L_c = L_{xc} e_1 + L_{\bar{y}c} e_2 + L_{\bar{z}c} e_3 \tag{20}$$

where the L_{jc}'s are given in Table 1. Equations (14) and (20) are added to yield the total angular momentum of the projectile:

$$L = L_x e_1 + L_{\bar{y}} e_2 + L_{\bar{z}} e_3 \tag{21}$$

where the L_j's are given in Table 1.

The differential equations for the angular motion are computed in the usual way.

$$\dot{L} \equiv \dot{L}_x e_1 + \dot{L}_{\bar{y}} e_2 + \dot{L}_{\bar{z}} e_3 + \Omega \times L = M_x e_1 + M_{\bar{y}} e_2 + M_{\bar{z}} e_3 \tag{22}$$

The roll equation is obtained from the first component of Eq. (22):

$$\dot{L}_x B_\gamma(\tilde{q} \sin\theta_\gamma - \tilde{r} \cos\theta_\gamma)\gamma + m_c x_c \dot{\theta}(\tilde{q} \sin\theta_\epsilon - \tilde{r} \cos\theta_\epsilon)\epsilon = M_x \tag{23}$$

The transverse angular motion equation is obtained by multiplying the third component of Eq. (22) by i and adding the result to the second component. If we retain only terms linear in Q, ϵ, and γ, L_x is replaced by L_{x0} and

$$I_t \dot{Q} - iL_{x0} Q + \dot{\Gamma} + \dot{E} = M_{\bar{y}} + iM_{\bar{z}} \tag{24}$$

The usual linear aerodynamic moment about the c.m. of the body can be written in the form‡

$$M_x = \tfrac{1}{2} \rho S l V^2 C_{l_p}(p_b l/V) \tag{25}$$

$$M_{\bar{y}} + iM_{\bar{z}} = \tfrac{1}{2} \rho S l V^2 \{[(p_b l/V) C_{M_{p\alpha}} - iC_{M_\alpha}]\xi + C_{M_q}(Ql/V) - iC_{M_{\dot{\alpha}}}(\dot{\xi} l/V)\} \tag{26}$$

‡More precisely, the moment about the c.m. of the combination should be used, but these two centers differ by the very small lever arm ϵ_b.

A good approximate relation between Q and $\bar{\xi}$ is[6]

$$iQ=\dot{\bar{\xi}}+(\rho SV/2m)C_{L_\alpha}\bar{\xi} \tag{27}$$

The small lift term can be neglected when we use this relation in the roll equation, but that term does have a damping effect on the complex angle-of-attack equation. Equations (25-27) can now be used to write Eqs. (23) and (24) in their final forms:

$$\dot{L}_x-A_{l_p}p_b+B_\gamma(\dot{\tilde{\beta}}\cos\theta_\gamma+\dot{\tilde{\alpha}}\sin\theta_\gamma)\gamma + m_c x_c\dot{\theta}(\dot{\tilde{\beta}}\cos\theta_\epsilon+\dot{\tilde{\alpha}}\sin\theta_\epsilon)\epsilon=0 \tag{28}$$

$$I_t\ddot{\bar{\xi}}-(A_q+iL_{x0})\dot{\bar{\xi}}-(A_\alpha+iA_{p\alpha})\bar{\xi}+i(\dot{\Gamma}+\dot{E})=0 \tag{29}$$

Quasilinear Solution

Equations (28) and (29) are nonlinear equations in $\tilde{\alpha}$ and $\tilde{\beta}$ since θ, the orientation angle of the angle-of-attack plane, is a nonlinear function of $\tilde{\alpha}$ and $\tilde{\beta}$. For a rigid body, $\epsilon=\gamma=0$, the equations become linear and the complex angle-of-attack motion is described by an epicycle determined by the equations

$$\bar{\xi}=\delta e^{i\theta}=(K_1e^{i\phi_1}+K_2e^{i\phi_2}) \tag{30}$$

$$K_j=K_{j0}\exp(\lambda_j t)\qquad j=1,2 \tag{31}$$

$$\phi_j=\phi_{j0}+\dot{\phi}_j t\qquad \dot{\phi}_1>\dot{\phi}_2 \tag{32}$$

$$\dot{\phi}_j=[L_{x0}\pm(L_{x0}^2-4I_tA_\alpha)^{1/2}]/2I_t \tag{33}$$

$$\lambda_j=(A_q\dot{\phi}_j+A_{p\alpha})/(2I_t\dot{\phi}_j-L_{x0}) \tag{34}$$

In Ref. 8, the quasilinear solutions for Eqs. (28) and (29) are obtained after considerable algebraic work. Most of this effort can be avoided by the observations that the two frequencies in the epicyclic motion of a spin-stabilized shell are usually quite different in magnitude and that the *derivatives* of θ, $\tilde{\alpha}$, and $\tilde{\beta}$ appear in the internal component terms of Eqs. (28) and (29). Thus, a good approximation can be obtained by considering only the high-frequency component of the pitching and yawing motion. Geometrically, this is equivalent to assuming that the internal motions have a fixed phase with respect to the high-frequency component of the shell's angular motion ($\theta=\phi_1$).

Equation (29) then reduces to

$$I_t\ddot{\bar{\xi}}-(A_q+iL_{x0})\dot{\bar{\xi}}-(A_\alpha+iA_{p\alpha})\bar{\xi}=(C_1+iS_1)\dot{\phi}_1\exp(i\phi_1) \tag{35}$$

Equation (35) can be easily solved by assuming a solution with the form of Eq. (30) and solving for the unknown functions ϕ_j and K_j. As might be expected, the equations for the slow-mode frequency and amplitude, $\dot{\phi}_2$ and K_2, are unchanged, while different relations result for the fast mode. (These relations neglect small damping terms in the frequency equation.)

$$I_t\dot{\phi}_1^2-(L_{x0}-C_1K_1^{-1})\dot{\phi}_1+A_\alpha=0 \tag{36}$$

$$\dot{K}_1=[(A_q\dot{\phi}_1+A_{p\alpha}-I_t\ddot{\phi}_1)K_1+\dot{\phi}_1S_1]/(2I_t\dot{\phi}_1-L_{x0})$$

$$\doteq\lambda_1K_1+\dot{\phi}_1S_1(2I_t\dot{\phi}_1-L_{x0})^{-1} \tag{37}$$

The internal component terms with ϵ and γ that appear in the roll equation [Eq. (28)] are all periodic in $\phi_1-\phi_2=\hat{\phi}$. Since we are primarily interested in the average variation of the spin and not the detailed small amplitude oscillation about this average, Eq. (28) can be replaced by its average over a cycle of the difference frequency $\hat{\phi}$.

$$\dot{L}_{x0}=A_{l_p}p_b-\dot{\phi}_1K_1S_1 \tag{38}$$

This equation shows that coupling between pitching motion and spin exists when the product of the fast-mode motion amplitude and S_1 is large enough.

Discussion

The ball fuze is a case where the c.m. motion can occur, but we can assume $\gamma=0$ and $p_b=p_c$. Equations (37) and (38) become

$$\dot{K}_1=\lambda_1K_1+\dot{\phi}_1^2m_cx_c\epsilon\sin\phi_\epsilon[2I_t\dot{\phi}_1-I_xp_b]^{-1} \tag{39}$$

$$I_x\dot{p}_b=A_{l_p}p_b-\dot{\phi}_1^2K_1m_cx_c\epsilon\sin\phi_\epsilon \tag{40}$$

In all flights, K_1 remained less than 120 mrad and no spin-down moment could be observed.

In Fig. 3, $\dot{K}_1/K_1$ is plotted vs Mach number for the 20 mm shell T282E1 with and without the ball rotor. For Mach numbers below 2, the exponential damping is well-determined, but above this Mach number considerable scatter occurs. Projectiles whose fuzes did not have the ball rotor have damping rates that lie close to -7/s, while those with the rotor have values that are as much as 9/s greater (i.e., $+2$).

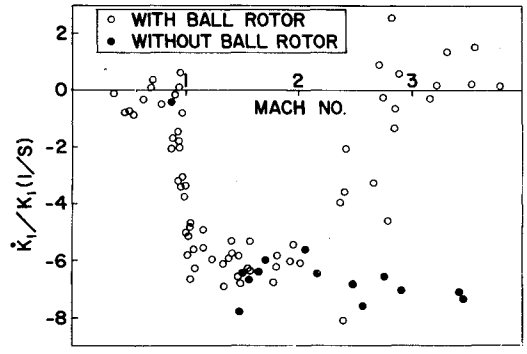

Fig. 3 Fast-mode damping rate for the 20 mm T282E1.

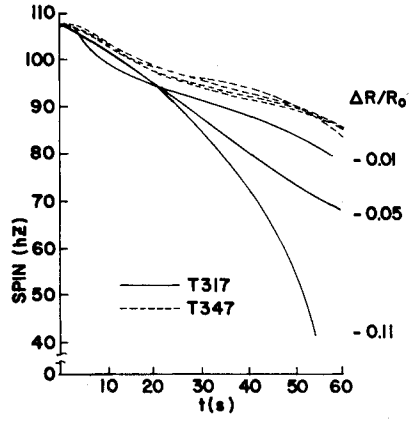

Fig. 4 Measured spin history of the T317.

Table 2 Parameters for T282E1 at Mach No. 3.3

$l=2.0$ cm	$C_D=0.41$
$m=96.6$ g	$C_{L_\alpha}=2.6$
$I_x=53.4$ g-cm^2	$C_M=2$
$I_t=394$ g-cm^2	$C_{M_q}+C_{M_{\dot{\alpha}}}=-5.3$
$m_c=3.0$ g	$C_{M_{p\alpha}}=0.15$
$x_c=2.9$ cm	
$V_0=1140$ m/s	
$p_0=1900$ Hz	

Table 3 Parameters for T317

$I_x/I_t = 0.1352$	0.218	M < 0.88
	$C_D =$ −0.9612 + 1.34M	0.88 ≤ M ≤ 1.1
	0.6503 − 0.125M	M > 1.1
$I_{xc}/I_t = 0.0472$		
$I_{tc}/I_t = 0.0251$		
	4.4	M < 0.88
	$C_{M_\alpha} =$ 1.32 + 3.5M	0.88 ≤ M ≤ 1.1
	5.17	M > 1.1
$C_{D_{\delta^2}} = 3$		
$C_{l_p} = -0.012$		
	$C_{M_{p\alpha}} = -0.26 + 9\delta^2$	δ < 0.1
	$-0.017\,\delta^{-1}$	δ ≥ 0.1
$C_{L_\alpha} = 2.0$		
$C_{M_q} + C_{M_{\dot\alpha}} = -6.3$		

Table 4 Verification of Eq. (42)

	Round 1 ($\gamma = 0.0037$)			Round 2 ($\gamma = 0.0035$)			Round 3 ($\gamma = 0.0254$)		
t, s	p_b, Hz	K_1, deg	$\sin\phi_\gamma$	p_b, Hz	K_1, deg	$\sin\phi_\gamma$	p_b, Hz	K_1, deg	$\sin\phi_\gamma$
0	108			135			108		
5	105	4	0.48	133	3	0.44	79	24	0.46
10	99	6	0.62	127	5	0.44	52	31	0.41
15				120	9	0.47	35	40	0.40
20				113	13	0.55	26	42	0.38
25	78	20	0.62						
30	69	24	0.62	96	19	0.44			
35	62	27	0.50	88	20	0.43			
40	60	27	0.50	80	20	0.61			

This phenomenon for Mach numbers near 2 can be ascribed to the action of a locking spring which releases the ball when the shell spin rate is large enough. For a given twist gun tube and air temperature, the initial spin rate is proportional to the launch Mach number.

The appropriate parameters for the T282E1 at Mach number 3.3 are given in Table 2. For Mach numbers between 2.8 and 3.8, measured K_1 falls between 0.05 and 0.12. The observed damping rate discrepancies can be explained by Eq. (39) with values of $\epsilon \sin\phi_\epsilon$ between 0.09 and 0.28 mm. These values are possible for the actual tolerances observed in this shell.

The actual spin histories of several T317s are given in Ref. 4 and are repeated as Fig. 4. This figure also gives the spin history for three T347s. The T347 shell has the same external shape, mass, and moments of inertia, but no movable internal components. In all observed cases, the T317 had a greater spin loss and flew to a lesser range. The relative decrements between the range of each T317 shell and the average range of the T347s is given in the figure. Thus, a spin loss of almost 70 Hz was observed for a projectile that flew 11% short of its proper range.

Unfortunately, measurements of angular motion were not made. A range loss of 11% would, however, require an average angular motion amplitude of 10-15 deg. The shell's internal construction is fairly complicated, but can be theoretically approximated by a single ring freely sliding on a central shaft. The tolerances are quite small but are sufficient to allow the ring to cant at an angle as large a 0.004 rad. When the ring is fully canted, its c.m. is on the axis of the shell and, hence, ϵ is zero. For simplicity, we will assume that the ring is spinning with the shell. The fast-mode damping rate, as given by Eq. (37), becomes

$$\dot K_1 = \lambda_1 K_1 + \dot\phi_1 (I_{xc} p_b - I_{tc}\dot\phi_1)\gamma \sin\phi_\gamma [2I_t\dot\phi_1 - I_x p_b]^{-1} \quad (41)$$

The spin equation [Eq. (36)] now reduces to

$$I_x \dot p_b = A_{l_p} p_b - \dot\phi_1 K_1 (I_{xc} p_b - I_{tc}\dot\phi_1)\gamma \sin\phi_\gamma \quad (42)$$

For a dynamically stable shell, λ_1 is negative. If ϕ_γ is in the first or second quadrant, the second term in Eq. (43) is positive and, hence, K_1 should grow to some equilibrium value. This equilibrium value of K_1 can then be used in Eq. (42) to give a spin-down moment. Our theoretical model of the behavior of the T317 is based on the assumption that it has values of γ and ϕ_γ, such that its fast-mode motion grows to 10-15 deg and causes the observed range loss and spin-down.

As a check on this conjecture, Eqs. (28) and (29) were coded for a digital computer. Although the complete set of aerodynamic coefficients are not well-known for this shell, nominal values were used and are given in Table 3.§ Figures 5 and 6 give the yawing motion and spin for the completely rigid shell ($\gamma = 0$). The yawing motion shows the usual small amplitude, slow-mode limit cycle which is frequently observed.

Computer runs were then made for $\gamma = 0.004$, $\phi_\gamma = 45$ deg. Figure 7 shows a rapid growth of the fast-mode angular motion to about 18 deg and a decay on the down-leg of the trajectory. A range loss of 11% was computed and a large spin-down is shown in Fig. 6. The computed spin-down is as large as the observed spin-down, but different in detail. Thus, we would assume that the actual angular motion grew much slower than our computed motion, but reached a much larger maximum value.

In summary, the theory gives good qualitative agreement with the observed behavior of the T317. In view of the in-

§Since a nonlinear Magnus moment was used in the numerical work, Eq. (37) no longer applies, but a quasilinear form of this equation can be obtained by the usual techniques.[6]

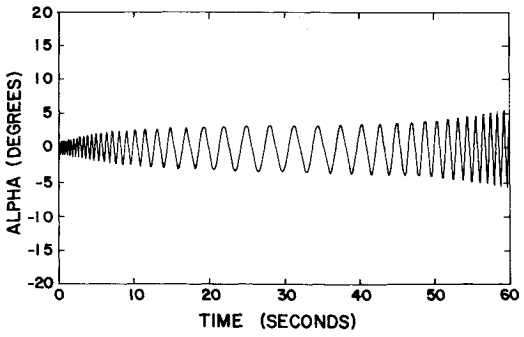

Fig. 5 Computed angular motion for the T317 ($\gamma = 0$).

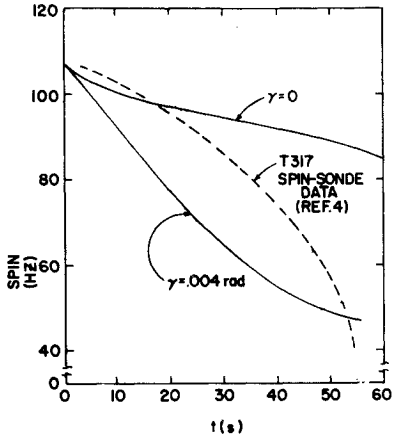

Fig. 6 Computed spin history for the T317.

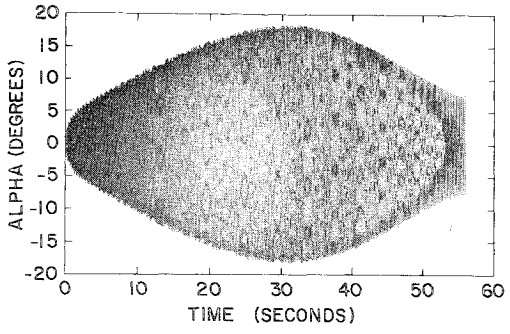

Fig. 7 Computed angular motion for the T317 ($\gamma = 0.004$).

complete information on its aerodynamic properties and angular motion, better quantitative results cannot be expected.

Recently, some additional firings of modified versions of the T317 have been made. These rounds were fired with different clearances and from guns with different twists. All were instrumented with sunsondes and telemetry units, so that continuous records of both the spin and the pitching motion were available.[9] Since A_{l_p} is well-known for this shell, these records can be used to verify Eq. (42).

Measurements of p_b, $\dot{p}_b$, K_I, $\dot{\phi}_I$ were taken at 5-s intervals and values of $\sin\phi_\gamma$ computed. Results from three rounds are given in Table 4. Rounds 1 and 2 have about the same clearances, but were fired from guns with different twists. Round 3 was fired from the same gun as round 1, but has a clearance seven times bigger than that of round 1.

We see that for all cases $\sin\phi_\gamma$ lies between 0.38 and 0.62. Since the phase angle is determined by the detailed interaction between the projectile and the internal part, there is no reason to expect it to remain constant. Its restriction to the range 22-38 deg, while the spin varies from 135 to 26 Hz and K_I varies from 3 to 42 deg, is very encouraging.

Conclusions

A theory has been developed for the motion of a projectile with a moving internal component that performs either a forced c.m. motion or a forced precession of its spin axis. According to this theory, the ball rotor rolls around the interior of its slightly oversized cylindrical cavity at a constant phase angle with respect to the plane of the angle of attack, thereby decreasing the damping rate of the fast-mode motion. In the case of the T317, the ring cants on a central column and spins at the gun launch spin rate, and the plane of the cant follows the angle-of-attack plane. The effect of this forced gyroscopic motion is to cause the fast-mode motion to grow to values in excess of 20 deg and thereby induce a rapid spin-down.

Acknowledgment

This theoretical work has benefited greatly from discussions with W. Chadwick and W. Soper[10] of the Naval Surface Weapons Center, H. Vaughn of Sandia Labs., and E. Freedman and J. Bradley of ARRADCOM.

References

[1] Boyer, E.D., "Comparison of Aerodynamic Characteristics of 20mm HEI Shell M97 with Fuze M75 and 20mm Shell T216E1 with Fuze M505," U.S. Army Ballistic Research Labs., Memo. Rept. No. 865, AD 69009, April 1955.

[2] Boyer, E.D., "Aerodynamic Characteristics for Small Yaws of 20mm Shell, HEI, T282E1 with Fuze M505 for Mach Numbers .36 to 3.78," U.S. Army Ballistic Research Labs., Memo. Rept. No. 916, AD 77515, Aug. 1955.

[3] Roecker, E.T. and Boyer, E.D., "Aerodynamic Characteristics of 30mm HEI Shell, T306E10," U.S. Army Ballistic Research Labs. Memo. Rept. No. 1098, AD 152952, Aug. 1957.

[4] Karpov, B.G. and Bradley, J.W., "A Study of Causes of Short Ranges of the 8″ T317 Shell," U.S. Army Ballistic Research Labs. Rept. No. 1049, AD 377548, May 1958.

[5] Hodapp, A.E., "Equations of Motion for Constant Mass Entry Vehicles with Time Varying Center of Mass Position," Sandia Labs. SC-RR-70-691, Nov. 1970.

[6] Murphy, C.H., "Free Flight Motion of Symmetric Missiles," U.S. Army Ballistic Research Labs. Rept. No. 1216, AD 442757, July 1963.

[7] Goldstein, H., *Classical Mechanics,* Addison-Wesley Publishing Co., Inc., Reading, Mass., 1950.

[8] Murphy, C.H., "Angular Motion of Projectiles with a Moving Internal Part," U.S. Army Ballistic Research Labs. Memo. Rept. No. 2731, AD A037338, Feb. 1977.

[9] Mermagen, W.H., "Measurements of the Dynamic Behavior of Projectiles over Long Flight Paths," *Journal of Spacecraft and Rockets,* Vol. 8, April 1971, pp. 380-385.

[10] Soper, W.G., "Projectile Instability Produced by Internal Friction," *AIAA Journal,* Vol. 16, Jan. 1978, pp. 8-11.